

The surface physics of ice in thunderstorms

J.G. Dash and J.S. Wettlaufer

Abstract: Laboratory and field studies have shown that thunderstorm electrification is principally due to rebounding collisions between ice particles and hail. Recent studies have provided clues for an understanding of the microphysics of the charging mechanism, involving the dynamics of vapor growth, molecular diffusion, and collisionally modified surface melting. The theory is in quantitative agreement with the systematic dependence of charge and mass transfer on growth rate, collision speed, and temperature.

PACS Nos.: 05.70-a, 64.10+h, 64.70-p, 63.35

Résumé : Les mesures en laboratoire et in situ ont montré que l'électrification dans les cellules orageuses est due aux collisions à ricochet entre les particules et la grêle. Des études récentes nous fournissent des indices sur la micro-physique du mécanisme de charge, impliquant la dynamique de la croissance de vapeur, la diffusion moléculaire et la modification par collision de la surface de fonte. La théorie agréée quantitativement avec la dépendance systématique de transfert de charge et de masse sur le taux de croissance, la vitesse de collision et la température.

[Traduit par la Rédaction]

1. Introduction

The study of thunderstorms has revealed considerable details of their electrical nature [1]. The anatomy of a common thunder cloud shows a principally dipolar charge distribution, having a positively charged upper portion and a negative lower region. Negative lightning strokes originate in this layer, where active ice is generated. Many simulation experiments indicate that collisions between small ice particles and hail can account for the observed electric fields. The principal features collected from field and laboratory studies are illustrated in Figs. 1*a* and 1*b*. Various mechanisms have been proposed to interpret the laboratory studies of collisional charging, but with limited success in modeling the complex dependence on environmental conditions [2]. However, a recent experiment [3], hereafter referred to as MD, has provided additional clues, leading to a detailed theory of the molecular process [4]. The theory describes collisional charging as a three-part sequence; before collision, contact, and separation. Drawing on the fields of surface physics and chemistry, the theory treats each stage in terms of the molecular dynamics of the ice interfaces. In the following sections we outline the theory and compare its predictions with laboratory results and storm measurements.

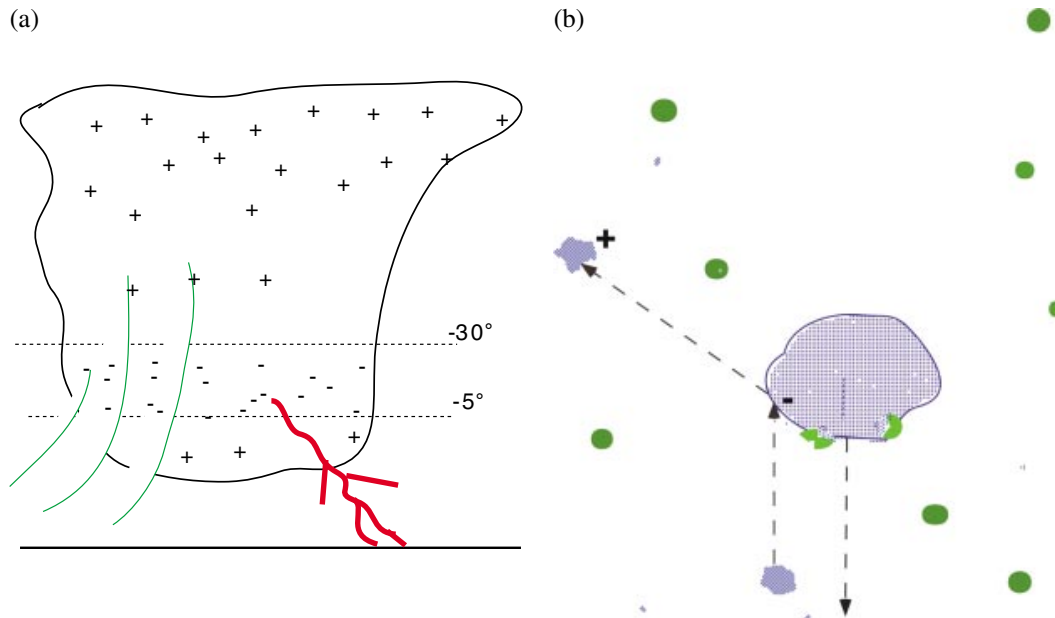
Received 15 July 2002. Accepted 17 November 2002. Published on the NRC Research Press Web site at <http://cjp.nrc.ca/> on 27 March 2003.

J.G. Dash.¹ Department of Physics, University of Washington, Seattle, WA 98195-1560, U.S.A.

J.S. Wettlaufer. Department of Geology and Geophysics and Department of Physics, Yale University, New Haven, CT 06520-8109, U.S.A.

¹Corresponding author (e-mail: dash@phys.washington.edu).

Fig. 1. (a) Anatomy of a typical thunderstorm, showing a principally dipolar charge distribution. Negative lightning-to-ground strokes originate in a region of active ice formation, where temperature ranges between -5°C and -30°C . (b) Charging takes place in collisions between small ice particles rising in updrafts and falling hail, in a background of super-cooled water droplets. The figure illustrates the dominant polarity resulting from ice-graupel collisions in storms with negative cloud-to-ground lightning.



2. Theory

2.1. Before collision: crystal growth

The electrical nature of the ice particles stems from their growth history before collision. Well-ordered crystals can be grown from vapor if the growth rate is slow enough for the deposited molecules to diffuse on smooth-surface facets to well-separated attachment sites at steps, kinks, and ledges. However, if the deposition rate is too fast the molecules will nucleate into clusters at shorter distances, a process known as kinetic roughening [5]. The scale of roughness is set by a competition between the deposition rate and surface diffusion. The average time τ between arrivals of vapor molecules at a surface site is related to the molecular site area a and deposition rate F by $\tau = (aF)^{-1}$. If the surface-diffusion coefficient is D_s , then, during τ , a freshly deposited molecule travels an average distance $\lambda = (2D_s\tau)^{1/2}$ before being buried by another molecule from the vapor [6]. Therefore, the average distance between clusters on a facet is

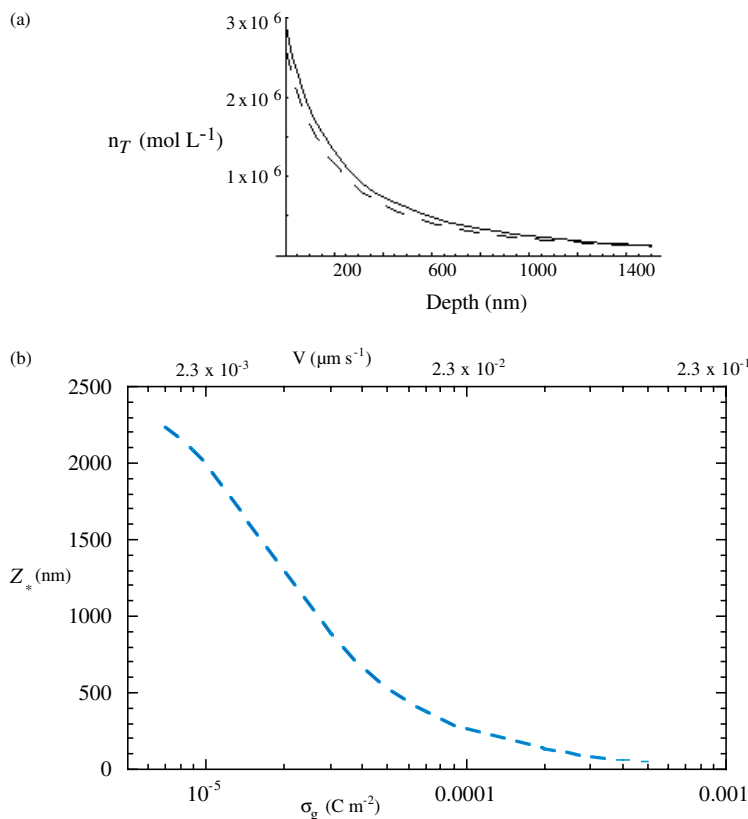
$$\lambda = \sqrt{\frac{2D_s}{aF}} \quad (1)$$

In the case of ice, disordered surfaces contain ionic defects at corners and edges. The ionization leaves OH^- ions bound to the site by their remaining hydrogen bonds, while the mobile positive ions diffuse deeper into the ice, thus creating a charged double layer and a negative surface potential. The surface-charge density σ_s is proportional to the surface-defect density. With (1), we have

$$\sigma_s = \frac{\xi e}{\lambda^2} = \frac{\xi eaF}{2D_s} \quad (2)$$

where e is the elementary charge. The empirical parameter ξ , responsible for the equality in the second part of the equation, is the surface structural-disorder factor, which can depend on growth conditions

Fig. 2. (a) Calculated charge density versus distance from the surface. The ordinate is the net-positive-charge density; $n_T = n_+ - n_-$. The negative charge is localized at the surface. The curves are calculated for a surface-charge density comparable to that of the MD experiments, at temperatures between -5°C and -20°C , using Gouy–Chapman theory [4]. To bound the possible behavior of growth-induced disorder, we show plots with a background ion density of $1.7 \times 10^{-7} \text{ ML}^{-1}$ (continuous curve) and $1.7 \times 10^{-11} \text{ ML}^{-1}$ (broken curve), which span the range from bulk water to bulk ice and we observe little quantitative difference in the profiles. (b) The calculated effect of growth rate V on the depth of the positive-charge distribution. Z is the depth at which the net ion density n_T reaches $1/e$ of its value at the interface. The surface-charge density σ_g is proportional to the growth rate.



and history. Comparison with laboratory results yields the empirical value $\xi = 4$ for the conditions of the MD study.

The charged double layer in the ice is similar to the phenomenon of an ionized surface in liquid water [7,8]. The diffusion of ions into the bulk is driven by the entropy available in the larger number of sites in the interior, and is opposed by the electrostatic field between the two distributions. This competition produces a concentration profile characterized by a Debye length

$$\kappa^{-1} = \left(\frac{\epsilon \epsilon_0 k_B T}{e^2 n} \right)^{1/2} \quad (3)$$

where k_B is Boltzmann's constant, ϵ is the dielectric constant of the medium, ϵ_0 is the vacuum permittivity, and n is the background density of counterions. The results of a detailed calculation of the distribution and its dependence on growth rate [4] are shown in Figs. 2a and 2b.

2.2. During contact: collisional melting

The impact between two ice particles causes temporary melting of a thin interfacial region. The effect of the impact is to enhance *premelting*, which is an otherwise equilibrium property of solid interfaces. In the *surface melting* of typical materials, the interface between a solid and vapor is wetted by a molecularly thin layer of melt liquid at a temperature below the bulk transition temperature T_0 , which then thickens as the temperature rises [9]. In some materials, surface melting begins as low as $0.8T_0$ but in ice without impurities the start is only a few degrees below 0°C . Variants of surface melting occur at interfaces between a solid and a foreign substance, and at grain boundaries between crystals of the same substance. Surface melting is enhanced by damage and other forms of disorder, which increase the chemical potential of the solid. In collisional melting, the premelting of the damaged region is proportional to the local disorder created by the collision. A quantitative estimate is derived by an extension [4] of the equilibrium theory of surface melting [9]. An estimate of the melt thickness d_m is given by a simple expression

$$d_m = \Delta E / Aqt \quad (4)$$

where ΔE is the inelastic energy deposit from the collision, A is the area of contact, q is the latent heat of fusion, and t is the reduced temperature relative to the melting point T_0 ; $t = (T_0 - T) / T_0$.

Equation (4) for the *damage-assisted* melt thickness was derived by an extension of the equilibrium theory of surface melting [4]. The theory predicts that damage incurred in ice–ice collisions can cause melting of many molecular layers at temperatures well below 0°C . It provides a quantitative explanation for the measured mass transfer in ice–ice collisions in the MD study. Collisional melting between two ice particles destroys the site bonds of the surface OH^- ions, and allows them to diffuse in the liquid layer. The brief time of contact, about 0.1 ms in the MD study, is sufficient for complete mixing of the OH^- ions, but too short for most of the positive ions to escape from their deeper sites in the solid. The contact is also too brief to allow much refreezing of the collisionally melted liquid.

2.3. Withdrawal: division of charge and mass

As two ice particles separate they take roughly equal shares of the collisionally melted liquid. The precise division will depend on details such as local shape and surface roughness, so that the sharing can only be estimated as a statistical average. Accordingly, in an average encounter, the particles share the liquid mass, together with its dissolved ions, so that the particle that had been growing more rapidly before the collision loses a greater number of its surface ions, and thus leaves the collision with a net positive charge.

The mass transfer depends on the ice particles' initial temperature difference. In typical cases, the colliding particles have quite different histories; the more rapidly growing particle having been colder. Assuming equal sharing of the impact energy loss, (4) predicts that the colder particle suffers less collisional melting. Consequently, when the melted liquid is shared, the colder particle comes away with some of the warmer particle's mass.

3. Comparisons with observations

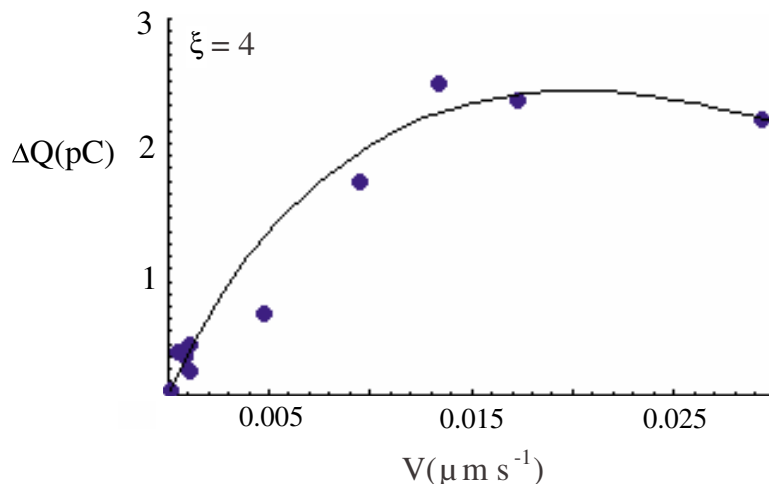
3.1. Laboratory measurements of collisional charging

Several significant features of laboratory measurements are explained by the theory, as follows.

3.1.1. Charge polarity

One of the strongest clues that helped in the development of the theory was a conclusion drawn from a collisional-charging study where the particle that had been undergoing more rapid vapor growth is charged positively [10]. The finding has been confirmed in several subsequent experiments [11].

Fig. 3. Charge transfer versus growth rate calculated from theory and compared with MD data. ΔQ is the charge on the experimental-collision area (10^{-8} m^2) [4].



3.1.2. Dependence of charge on growth rate

The MD study showed that the charge transfer is proportional to the rate of growth at low rates, but increases more slowly and declines at increasingly high growth rate. These results are shown in Fig. 3, together with a theoretical curve. The agreement is obtained by fitting a single adjustable constant, the surface structural-order parameter ξ . We note that ξ is not simply a scaling parameter, for it appears in the theory in an essentially transcendental way.

A significant feature of the measurements is the decrease of the charging “efficiency” at high growth rates, i.e., the curve of charge *versus* growth rate falls below a linear dependence at high rate, and even begins to decrease. The entire curve is explained by the theory. The linear portion at low rates is explained by the proportionality of surface-charge density on growth rate. At increasingly high growth rates the greater electric field between the positive- and negative-charge distributions causes a contraction of the positive distribution toward the surface. Due to its shallower depth, during a collision a larger fraction of the positive charge is liberated into the melt layer, thereby neutralizing more negative charge.

3.1.3. Identification of the mobile charge

Positive charging of the faster grown particle can be caused by acquisition of positive ions or by a loss of negative ions. Experiments on collisional charge transfer between ice particles and between ice and other materials has indicated that the transferred charge is negative [12]. The theory agrees, in that the positive charging is due to the loss of OH^- ions.

3.1.4. Linkage of surface charge and disorder

Experiments have shown that ice surfaces that have been damaged by abrasion or subjected to rapid growth by riming have large negative surface potentials [13]. The theory is in agreement: ionization is caused by kinetic roughening, and the separation of positive and negative charges results in a negative surface polarity. *Mass transfer*: the MD experiment shows that mass transfer accompanies charge transfer, the colder particle gaining an amount of mass roughly proportional to the temperature difference. The theory is in quantitative agreement with the measured mass transfer. *Fluidity of transferred mass*: the MD experiment indicated that the mass exchanged during collisions was fluid-like rather than solid fragments, even at temperatures as low as -16°C . This was an important clue in the development of the theory, for it could not be explained in terms of equilibrium-surface-melted fluid. It eventually led to an extension of the theory to impurity effects and collisional melting.

3.2. Comparisons with storm measurements

Thunderstorm dynamics indicate that small growing particles rising in updrafts are positively charged, and that the negative charges are on falling graupel particles. The theory of collisional charging explains this polarity as due to faster vapor growth on the small particles. At present, this interpretation is only a presumption, for the two particles grow by complicated mechanisms. The small particles probably experience rapid vapor growth immediately after freezing is nucleated, with a sudden burst of vapor when its temperature rises and then falls. Freezing occurs during their ascent; vapor growth then results from recapture of some of the particle's vapor and condensation from super-cooled liquid droplets. The falling graupel, on the other hand, can grow by riming. The impact of super-cooled liquid droplets nucleates freezing, which causes a sudden rise of temperature to the ice point, and a quick burst of vapor. A detailed calculation, [10], shows that an appreciable fraction of the vapor recondenses on the graupel near the impact site. Depending on the surface temperature, the condensation can be very rapid. The collision region is, therefore, a mixture, where small particles and graupel can have either polarity, depending on their immediate histories and the details of their collisions. Such a mixture has been concluded from storm measurements [1], and is illustrated in Fig. 1*b*. The average charge density measured in typical storms is a result of the quantitative difference between the populations. Judging the dominant polarity of collisional charging from the fact that most storms produce negative lightning from their lower regions, Fig. 1*b* shows a representative case. In less common storms, positive lightning originates in lower layers of the cloud. This can be due to differences in cloud conditions, although the basic physics of collisional charging remains the same.

The theory requires temporary melting during contact to allow appreciable charge transfer. Model calculations confirm that collisional melting occurs at typical collision speeds and temperatures. Calculated melt thickness in collisions between ice spheres and a plane are given below. The thickness d_m is given in molecular layers, the sphere radius R in micrometres, and the approach speed V in m s^{-1} : $R = 10$, $V = 1$, $T = -35^\circ\text{C}$, and $d_m = 6$; $R = 25$, $V = 3$, $T = -15^\circ\text{C}$, and $d_m = 40$; $R = 50$, $V = 10$, $T = -5^\circ\text{C}$, and $d_m = 500$. From these values one sees that the melt thickness is very small at low velocities and temperatures. This provides a reason for the lower temperature limit of a thunder cloud's active charging region.

4. Conclusion

The collisional charging of ice, which is believed to underlie the process of electrification of thunderstorms, involves the molecular and surface physics of ice. A quantitative theory links laboratory measurements of mass and charge transfer with growth and damage-assisted surface melting. Further development of the theory, together with new measurements can improve the approximations, and new laboratory experiments can test its assumptions and lead to refinements. The ideas can be tested by incorporation of the collisional-charging results into a cloud dynamical model. Finally, the extensions of the equilibrium theory may be applicable to other ice phenomena.

Acknowledgements

This research is supported by the Leonard X. Bosack and Bette M. Kruger Foundation and by the National Science Foundation.

References

1. D.R. MacGorman and W.D. Rust. The electrical nature of storms. Oxford University Press, New York. 1998.
2. C.P.R. Saunders. J. Geophys. Res. **99**, 10773 (1994).
3. B.L. Mason and J.G. Dash. J. Geophys. Res. **105**, 10185 (2000).
4. J.G. Dash, B.L. Mason, and J.S. Wettlaufer. J. Geophys. Res. **106**, 20395 (2001).

5. R.W. Smith and D.J. Srolovitz. *J. Appl. Phys.* **79**, 1448 (1996); J. Krim and J. Palasantzas. *Int. J. Mod. Phys.* **9**, 599 (1995).
6. A. Einstein. *In* Investigations on the theory of Brownian movement. Dover, New York. 1956. pp. 1–18.
7. E.J.W. Verwey and J.Th.G. Overbeek. *Theory of stability of lyophobic colloids.* Elsevier, Amsterdam. 1948.
8. J.M. Israelachvili. *Intermolecular and surface forces.* Academic Press, London. 1992. Chapt. 12.
9. J.G. Dash, H.-Y. Fu, and J.S. Wettlaufer. *Rep. Prog. Phys.* **58**, 115 (1995).
10. B. Baker, M.B. Baker, E.R. Jayaratne, J. Latham, and C.P.R. Saunders. *Q.J.R. Met. Soc.* **113**, 1193 (1987).
11. J.M. Caranti, E.E. Avila, and M.A. Re. *J. Geophys. Res.* **96**, 15365 (1991); C.P.R. Saunders and S.L. Peck. *J. Geophys. Res.* **103**, 13949 (1998); W.D. Keith and C.P.R. Saunders. *Atmos. Res.* **25**, 445 (1990).
12. E.R. Jayaratne. *Atmos. Res.* **26**, 407 (1991); E.R. Jayaratne. *J. Geophys. Res.* **103**, 13957 (1998).
13. J.M. Caranti and A.J. Illingworth. *J. Phys. Chem.* **87**, 4125 (1983).